Direct determination of Al and Pb in waste printed circuit boards (PCB) by Laser-induced breakdown spectroscopy (LIBS): evaluation of calibration strategies and economic - environmental questions

Diego Victor Babos,[1,2] Andrés Cruz-Conesa,[1] Edenir Rodrigues Pereira-Filho[2] and Jesús Manuel Anzano[1*]

[1]Laser Laboratory, Chemistry & Environment Group, Department of Analytical Chemistry, Faculty of Sciences, University of Zaragoza, Pedro Cerbuna 12, 50009 Zaragoza, Spain

[2]Group of Applied Instrumental Analysis, Department of Chemistry, Federal University of São Carlos, São Carlos, São Paulo State, 13565-905, Brazil

*Corresponding author:
Jesús Manuel Anzano
Laser Laboratory, Chemistry & Environment Group, Department of Analytical Chemistry, Faculty of Sciences, University of Zaragoza, Pedro Cerbuna 12, 50009 Zaragoza, Spain
Phone number: +34 9 7676 2684
E-mail: janzano@unizar.es (J. Anzano).

Graphical abstract

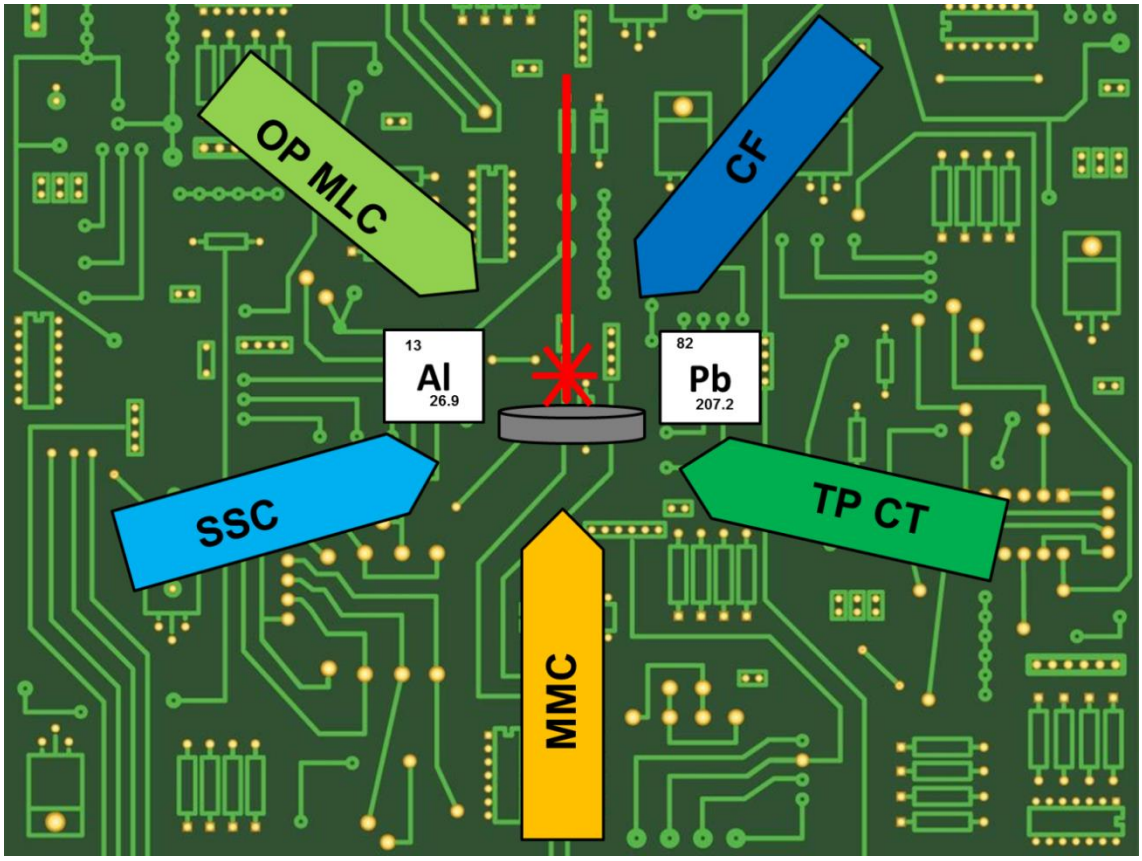

Evaluation of five calibration strategies for direct determination of recyclable and toxic metals in waste PCB by LIBS

Highlights

- Fast and direct determination of Al and Pb in waste PCB by LIBS
- Evaluation of five calibration strategies to overcome matrix effects by LIBS
- Recent calibration strategies by LIBS were applied to determine Al and Pb in WEEE.
- Pb concentration are 5 to 12 times higher than established by Directive 2011/65/EU

Abstract

Matrix-matching calibration (MMC), two-point calibration transfer (TP CT), one-point and multi-line calibration (OP MLC), single-sample calibration (SSC) and calibration free (CF) were evaluated in order to overcome matrix effects in laser-induced breakdown spectroscopy (LIBS). These calibration strategies were evaluated for direct determination of Al and Pb in waste printed circuit boards (PCB) using direct solids analysis by LIBS. Each strategy has limitations and advantages of its implementation, for the correction of matrix effects, so that it allows elementary determination with adequate accuracy. The MMC and CF proved to be excellent calibration strategies for the determination of strategic (Al) and toxic (Pb) elements by LIBS, with good recoveries (ranging from 80 to 120%) and low relative standard deviation (RSD%) values. A detailed discussion of the advantages and limitations of each of these five calibration strategies evaluated for LIBS is presented in this study. Lead concentrations in waste PCB samples are 5 to 12 times higher than established by Directive 2011/65/EU, and the samples analyzed contain between 3 and 55 g kg^{-1} Al, being an interesting economic and recycling source for this metal.

Keywords: WEEE; Toxic element; Environment pollution; Matrix-matching calibration; Two-point calibration transfer; Calibration free; Single-sample calibration; One-point multi-line calibration

1. Introduction

Contemporary society utilizes several types of high-tech electrical and electronic devices and instruments. The study of waste electrical and electronic equipment (WEEE) generation is therefore of great interest due to the environmental, economic, recycling and reuse questions posed by this type of waste (Costa et al. 2018a, Tansel, 2017). According to a study published in 2017, the projection of WEEE production is expressive (Andrade et al. 2019a, 2019b, 2019c, 2019d), being 52.2 million tons in 2021 (Baldé et al. 2017).

WEEE contains a diverse, complex and valuable composition, consisting mainly of polymers, metals (base, toxic, noble and technological elements) and ceramics. Printed circuit boards (PCB), which are part of the electronic devices present in the WEEE, contain large amounts of valuable and dangerous metals such as, for example, Al and Pb. Depending on the electronic device, the metal content on PCBs can range from 2 to 19% Al and 1 to 3% Pb, among others (Andrade et al. 2019b, Arshadi et al. 2018, Carvalho et al. 2015, Perkins et al. 2014, Yamane et al. 2011, Yang et al. 2019). Aluminum and Pb can be recycled, adding value to the WEEE and generating a source of income. Lead is a toxic metal which in high concentrations can pollute the environment. According to Directive 2011/65/EU, the maximum concentration allowed is 0.1% by weight in homogeneous materials (RoHS, 2011).

The preparation of waste PCB samples for elemental analysis is a challenging task due to the complexity of its composition and its refractory character, being rich in oxides of Mg, Si and Ti, flame retardants, metals and polymers. Thus, the need to use vigorous conditions in the acid decomposition step is evident in order to obtain a homogeneous and representative solution for

subsequent quantitative analysis by conventional analytical techniques (Arshadi et al. 2018).

LIBS technique has some advantages that could be used for the direct analysis of waste PCBs, such as: minimum sample preparation, fast multi-element analysis (μs), semi-destructive analysis (μg), and minimum waste generation. A limitation of this technique is related to matrix effects, which may compromise accuracy in quantitative analysis (Andrade et al. 2020, Carvalho et al. 2018a, Costa et al. 2019, Cremers and Radziemski 2006, Gondal et al. 2010, Kim et al. 2013, Lasheras et al. 2011, Miziolek et al. 2006).

As the sample is analyzed integrally (analyte and matrix simultaneously) by the LIBS instrument, the physicochemical properties of the sample and the laser-sample and/or laser-plasma interaction may influence the atomic/ionic/molecular emission phenomenon of the analyte (Cremers and Radziemski 2006a, Miziolek et al. 2006). As in the majority of applications the goal is quantitative analysis, requiring calibration standards in some strategies. In addition, different matrix effects can occur in the plasma formed in the samples and in the calibration standards. Consequently, the figures of merit of the method can be jeopardized, and thus may make it impossible to determine the analyte with satisfactory accuracy using direct solid analysis by LIBS (Hahn and Omenetto 2010, Hahn and Omenetto 2012, Sattar et al. 2019).

Matrix effects (spectral and non-spectral) can be avoided or minimized by careful peak selection or peak fitting of the analytical line and / or selecting lines that do not exhibit spectral interference, in addition the use of high resolution spectrometers in LIBS (makes it possible to identify and overcome some spectral interferences) (Takahashi and Thornton 2017, NIST).

The non-spectral matrix effects are directly correlated to the physical and chemical properties of the sample, and these effects are more difficult to overcome because there are many possibilities of how the matrix may be influenced by the analyte emission phenomenon (Cremers and Radziemski 2006a, Takahashi and Thornton 2017). The main non-spectral matrix effects are related to the sample's irregular surface, inhomogeneous particle size and humidity (Carvalho et al. 2018, Takahashi and Thornton 2017), the predominant chemical composition of the sample (organic or inorganic forms) (Eppler et al. 1996), the temperature of the sample (Lednev et al. 2019), the pressure used to compress the sample to form pellets (when necessary) (Popov et al. 2018), the presence of easily ionizable elements (EIEs) (Morais et al. 2018, Popov et al. 2018), the interaction of the laser with the sample, heat of vaporization, thermal conductivity, and the absorption coefficient, which affects the transport of an ablated mass which will be vaporized and atomized into the plasma (Takahashi and Thornton 2017), among others (Lasheras et al. 2013, Rezaei et al. 2018). These matrix effects may contribute to the non-stoichiometric ablation of the sample and thus reduce the possibility of using LIBS for quantitative analysis.

In order to overcome these matrix effects, univariate and multivariate calibration strategies are used for LIBS: matrix-matching calibration (MMC) (Costa et al. 2018b, Gomes et al. 2013, Vieira et al. 2018), standard addition (SA) (Yi et al. 2016, Wu et al. 2019), one-point gravimetric standard addition (OP GSA) (Babos et al. 2019), internal standardization (IS) (Aquino et al. 2016, Carvalho et al. 2018b, Lasheras et al. 2013, Sperança et al. 2019) calibration free (CF) (Calvacante et al. 2013, Ciucci et al. 1999, Li et al. 2019, Tognoni et al. 2010), one-point and multi-line calibration (OP MLC) (Hao et al. 2018), multi-

150 energy calibration (MEC) (Andrade et al. 2019b, Augusto et al. 2019, Babos et
151 al. 2018, Carvalho et al. 2019, Castro et al. 2020, Fortunato et al. 2019), two-
152 point calibration transfer (TP CT) (Castro et al. 2020), and single-sample
153 calibration (SSC) (Yan et al. 2019).

154 It should be noted that many calibration possibilities are available for
155 LIBS, but the question is what is the best calibration strategy that could be
156 applied for the determination of Al and Pb in samples as complex, of
157 environmental and economic interest as waste PCBs. In order to answer this
158 question, five calibration strategies were selected and evaluated their
159 performance based on various parameters such as standard error (SE),
160 recovery and other figures of merit, considering the limitations and intrinsic
161 advantages of each calibration for overcoming matrix effects and for the
162 determination of these metals. Two strategies widely reported in the literature
163 (MMC and CF) and three that have recently been proposed (TP CT, OP MLC
164 and SSC) for calibration were evaluated for direct waste PCB analysis and
165 determinations of toxic (Pb) and strategic (Al) elements by LIBS.

166 **2. Experimental**

167 2.1. Instrumentation

168 LIBS spectra were obtained using an experimental set-up based on a
169 Q-switched Nd:YAG laser (BrilliantQuantel, model Ultra CFR) with a 1064 nm
170 wavelength, a 7.7 ns pulse duration and a maximum laser pulse energy of 50
171 mJ. The sample was placed inside a sample chamber and the laser beam
172 directly focused on it through a 150 mm focal length lens. The target surface
173 was positioned approximately 77 mm below the focal lens. The light emitted by
174 the plasma was collected by optic fibers connected to an Echelle spectrometer

(Andor Mechelle ME5000, 195 mm focal length, F/7, l/Al 5000). The spectrometer is equipped with an intensified charge coupled device detector (Andor iStar DH734, 1024 × 1024 pixels 13.6 × 13.6 μm^2 by pixel, 18 mm of intensifier diameter). The wavelength and spectral resolution of the spectrometer were calibrated using a low pressure mercury-argon lamp by measuring both the spectral positions of the lines and their spectral profiles. The LIBS system requires some instrumental parameters to be optimized such as laser pulse energy, delay time, signal acquisition time and lens-sample distance.

An inductively coupled plasma optical emission spectrometer (ICP OES) (iCAP 7000, Thermo Scientific, Waltham, MA, USA) was used in the determination of Al and Pb in printed circuit board waste after acid digestion of the samples (n=3). The concentrations obtained were used as reference values for the LIBS method. The emission lines monitored during ICP OES determinations were Al 167.079 nm and Pb 216.99 nm using axial viewing mode.

A scanning electron microscope (SEM) (JEOL JSM 6360-LV) (General Research Support Service of the University of Zaragoza) with voltage up to 30 kV and a maximum resolution of 3.0 nm was used for the morphological surface visualization of the waste PCBs. In order to perform the analysis, one waste PCB sample was pelletized and selected (S2). Additionally, the pellet was analyzed by SEM in order to obtain information about the crater formed by the laser pulse and then to calculate both the irradiance and laser pulse fluence values.

2.2. Reagents and samples

Standard solutions containing Al and Pb were prepared by diluting standard stock solutions containing 1000 mg L^{-1} (Specsol, São Paulo, Brazil), and acidified with HNO_3 10% v v^{-1}, and used for ICP OES analysis.

Six PCBs from desktop computers were collected at São Carlos (São Paulo State, Brazil) and then ground in a knife mill (IKA, A11) (the particle size was estimated to be lower than 500 μm) to obtain homogeneous and representative samples. Approximately 200 mg of PCB samples were weighed and compressed using a manual hydraulic press (Perkin Elmer IR Accessory Hydraulic Press) with $10x10^4$ N for 2 min, to obtain pellets (n=3) for LIBS analysis. It is necessary to press the sample to obtain cohesive pellets that contribute to the reproducibility of the laser-sample interaction and consequently to the precision of the measurements.

2.3. Sample preparation for determination of Al and Pb by ICP OES

The samples of PCBs were digested using microwave-assisted heating for analysis and to obtain reference values of Al and Pb that were subsequently used in the proposition of the calibration models and verification of the accuracy of the proposed LIBS method. Masses of approximately 100 mg of PCB were accurately weighed directly in the perfluoroalkoxy alkanes (PFA) digestion vessels and microwave-assisted digested using a single reaction chamber oven (UltraWave™, Milestone, Sorisole, Italy). Volumes of 5 mL of concentrated HNO_3 were used as an oxidizing agent in the decomposition. The microwave heating program was applied as follows: (1) 5 min to reach 100 °C, (2) 15 min to reach 180 °C, (3) 15 min to reach 240 ºC and (4) 7 min held at 240 °C. Subsequently, the digests were diluted to 50.0 mL with distilled-deionized water

and filtered on qualitative filter paper 80 g m^{-2} (Unifil, Germany) for subsequent ICP OES analysis.

2.4. Optimization of LIBS instrumental parameters

Using a full factorial design 2^3 with center and axial points, the instrumental conditions (delay time, gate width and laser pulse energy) were optimized. The variables studied were evaluated at five levels: delay time (0.01, 0.4, 1.2, 2.0 and 2.54 µs), gate width (0.32, 1.0, 2.0, 3.0 and 3.68 µs) and laser pulse energy (20, 25, 35, 42.5 and 47.5 mJ). The variable levels were coded between -1.68 (lower level) and +1.68 (higher level), with the central point (coded as 0) used to calculate experimental errors. Table S1 presented at supplementary material shows more details about the experimental design performed. Due to experimental setup limitations the delay time values were coded from -1.49 (0.01 µs) to 1.68 (2.54 µs) The S2 waste PCB sample containing 55 ± 3 g kg^{-1} Al and 11.6 ± 0.8 g kg^{-1} Pb was used to optimize the instrumental conditions used in the LIBS analyses. The Al and Pb reference concentrations were obtained after microwave digestion and ICP OES determinations.

The signal-to-background ratio (SBR) calculated for each monitored emission line of Al and Pb (besides the lines of Ca, Fe, Si and Ti used for calibration free) were used as responses of the factorial design. A mathematical approach developed by Derringer and Suich (1980), based on desirability functions applied to optimize multi-response experiments, was used in this study. This strategy first converts each experimental response into an individual desirability value (d_i), which ranges between $0 \leq d_i \leq 1$. In this case, $d_i = 1$ corresponds to a desired response (high SBR), while $d_i = 0$ represents a

249 response that is outside the acceptable region (the lowest SBR). The individual
250 desirability value was combined into a single response after an arithmetic mean
251 calculation (the overall desirability, OD). In this study, was exceptionally used
252 the arithmetic mean because some experiments resulted in di = 0.

253 2.5. Calibration strategies

254 Five calibration strategies were evaluated for the determination of Al
255 and Pb in waste PCB samples by LIBS. For all the calibration strategies, the
256 calibration standards and samples were pelletized (n=3) using approximately
257 200 mg of waste PCB. The resulting pellets were analyzed using 50 pulses in
258 different spots to obtain a single average spectrum. For each sample, six
259 average spectra were obtained (total of 300 shots per sample).

260 Eight different strategies for normalization of the spectra (Castro and
261 Pereira-Filho 2016, Sperança et al. 2018) were evaluated. These normalizations
262 are important to minimize the signal fluctuations (area or height) and sample
263 matrix differences during data acquisition.

264 2.5.1 Matrix-matching calibration – MMC

265 For MMC method, calibration curves in the range from 3.1 to 55 g kg^{-1}
266 Al and 0.72 to 11.6 g kg^{-1} of Pb were obtained using four samples of waste
267 PCBs as solid standards. The curves were obtained by plotting the analytical
268 signal (y-axis emission intensity) *versus* the analyte concentration (x-axis).

269 Four emission lines with different relative intensities for Al (Al I 308.21
270 nm, Al I 309.40 nm, Al I 394.40 nm and Al I 396.15 nm) and two lines for Pb (Pb
271 I 363.95 nm e Pb I 405.78 nm) were evaluated to obtain the calibration curves.
272 The choice of the best normalization mode and the most appropriate emission
273 line was made using as a criterion the obtaining of calibration curves that

enable the smallest errors of prediction of the analyte concentration in the samples.

The concentration of the analyte, using MMC, is calculated using equation 1,

$$C_{analyte} = \frac{Intensity - intercept}{slope} \qquad \text{(Eq. 1)}$$

where $C_{analyte}$ is the concentration of Al or Pb determined in the sample, Intensity is the analytical signal of the emission line obtained, slope and intercept, both obtained by the calibration curve.

2.5.2. Two-point calibration transfer – TP CT

For TP CT only one sample is used as the calibration standard, and the linear model is obtained with two analytical signals monitoring only one analyte emission line. The linear model plot is made using two sets of spectra in the x-axis, and in the y-axis the intensity of the emission line is obtained using only the sum of the intensity of the spectra (height or signal area) through normalization 5.

Using the reference concentration ($C_{standard}$) of the analyte in the calibration standard, and the slopes obtained in linear models for the sample ($slope_{sample}$) and for the calibration standard ($slope_{standard}$), the analyte concentration ($C_{analyte}$) can be obtained using equation 2 (Castro et al. 2020).

$$C_{analyte} = \frac{slope_{sample}}{slope_{standard}} \times C_{standard} \qquad \text{(Eq. 2)}$$

For TP CT the emission lines Al I 396.15 nm and Pb I 405.78 nm were used to obtain linear models.

2.5.3. One-point and multi-line calibration – OP MLC

For the OP MLC, only one sample is used as the calibration standard and several emission lines are used to obtain calibration linear models for Al

and Pb. In the x-axis, the emission intensities are used for all the monitored analyte lines in the standard calibration, and in the y-axis the intensities are used for all the monitored lines in the sample.

The analyte concentration ($C_{analyte}$) is calculated using equation 3,

$$C_{analyte} = slope \times C_{standard} \quad \text{(Eq. 3)}$$

where the slope is obtained for the linear model, and $C_{standard}$ is the concentration of the analyte in the sample used as the standard calibration (Hao et al. 2018).

Using four atomic emission lines for Al (308.21nm, 309.27 nm, 394.40 nm and 396.15 nm) and two atomic emission lines for Pb (363.95 nm and 405.78 nm), linear models were obtained for each analyte in the respective samples.

2.5.4. Single-sample calibration – SSC

In the SSC method, only one sample is used as the calibration standard and several emission lines of the analyte present in the standard and sample (unknown) are used. The SSC does not require a calibration curve or linear models (Yan et al. 2019).

For this strategy, the emission intensities of Al I 396.15 nm, Pb I 405.78 nm and Mg II 279.55 nm were used to determine the concentration of the analyte. The S2 PCB sample containing 55 ± 3 g kg^{-1} Al, 11.6 ± 0.8 g kg^{-1} Pb and 11.4 ± 1.8 g kg^{-1} Mg (obtained after microwave digestion and ICP OES determination) was used as the calibration standard.

The analyte concentration ($C_{analyte}$) is calculated using equation 4,

$$C_{analyte} = \frac{\frac{C_{\,standard\ analyte} \times I_{analyte\ sample}}{I_{\,analyte\ standard}}}{\sum_{i=1}^{N} \frac{C^{N}_{standard\ element} \times I^{N}_{element\ sample}}{I^{N}_{element\ standard}}} \quad \text{(Eq. 4)}$$

where $C_{standard\ analyte}$ and $I_{analyte\ standard}$ are the concentration and intensity of the emission line of the analyte in the PCB sample, respectively, used as the calibration standard (#S2 PCB). The $I_{analyte\ sample}$ is the emission intensity of the analyte in the unknown sample. The $I^{N}_{element\ sample}$ is the emission intensity of the element N in the sample of unknown concentration, and $C^{N}_{standard\ element}$ and $I^{N}_{element\ standard}$ the concentration and the emission intensity of the element N, respectively, in the sample used as the standard calibration.

2.5.5. Calibration Free – CF

For CF only physicochemical parameters of the obtained plasma and from the monitored emission lines of the analytes and from all species present are necessary for the quantification. A calibration standard is not required.

The analyte concentration ($C_{analyte}$) is calculated using equation 5,

$$ln\frac{I_\lambda}{A_{ki}g_k} = ln\frac{C_{analyte}}{U(T)} - \frac{1}{K_B T}E_k \qquad \text{(Eq. 5)}$$

where I_λ is the integrated intensity of the emission line, A_{ki} the transition probability, g_k the degeneration of the upper level, K_B the Boltzmann constant, T the temperature of the plasma, E_k the energy level of the excited state, F the experimental factor, and U(T) the partition function of the species present in the plasma (Ciucci et al. 1999, Li et al. 2019, Tognoni et al. 2010,).

All the calculations were processed using the LIBS++ software (ARWAN technology, developed by Palleschi et al.). For the calculation of the plasma temperature, the emission lines for Ba (Ba I 705.99, Ba II 614.17 and Ba II 649.69 nm), Fe (Fe I 374.55, Fe I 382.04, Fe I 405.58, Fe I 438.35, Fe II 239.92 nm) and Ti (Ti I 498.17, Ti I 499.10 and Ti II 333.94 nm) were used.

The plasma electron density (N_e) was calculated from the Hα line in 656.28 nm and using Equation 6,

$$FWHA = 0.549nm \times \left(\frac{N_e}{10^{23}\, m^{-3}}\right)^{0.67965} \quad \text{(Eq. 6)}$$

where FWHA denotes the full width at half area of this hydrogen emission line (Cavalcante et al. 2013, Ciucci et al. 1999,).

Figure 1 show a pictorial description of all the calibration strategies (calibration curve, linear model or correlation) used for Al.

2.6. Determination of analytical performance parameters

The precision (n=3) was calculated using all the samples. The standard error (SE) and root mean square error of prediction (RMSEP) were calculated for analytes, using Equations 7 and 8, respectively:

$$SE = \sqrt{\frac{\sum(y_i - \hat{y})^2}{n-1}} \quad \text{(Eq. 7)}$$

$$RMSEP = \sqrt{\frac{\sum(y_i - \hat{y})^2}{n}} \quad \text{(Eq. 8)}$$

where y_i is the analyte reference concentration obtained by ICP OES, $\hat{y}$ is the concentration predicted by the calibration model using LIBS, and n is the number of samples analyzed.

Slope and intercept values and respective confidence interval (95 % confidence level) obtained for linear regression for concentration reference (ICP OES method) *versus* concentration predicted (LIBS method) plots, were used for results comparison obtained in the direct determinations of analytes using five calibration strategies for LIBS. The ideal situation is a slope and intercept equals to 1 and 0, respectively.

3. Results and discussion

3.1. Optmization of LIBS instrumental conditions

The instrumental conditions of the LIBS system influence the laser-matter interaction and also the quality of the emission spectrum obtained. The

372 laser pulse energy, delay time and gate width of the spectrometer were
373 optimized using a full factorial design 2^3 with center and axial points (see Table
374 S1).

375 The regression model based on the obtained OD (Table S1) was
376 calculated to determine the best description of the experimental region. The
377 quality of the model was evaluated through analysis of variance (ANOVA). After
378 observing the values calculated for ANOVA, it was possible to verify that the
379 regression of the model is not statistically significant at the 95% confidence
380 level. These results demonstrate that it is not possible to obtain a model with
381 good predictive capacity.

382 By evaluating Table S1, it was observed that experiment 8 presented
383 the highest OD value (OD = 0.89) when compared to the other experiments.
384 Thus, the evaluated conditions of this experiment were used in all
385 measurements by LIBS in this study, with a delay time of 2 µs, a gate width of 3
386 µs and laser pulse energy of 42.5 mJ.

387 3.2. Laser-sample interaction: energy parameters

388 The physical and chemical properties of the sample strongly influence
389 the laser-sample interaction and consequently the formation of the plasma,
390 modifying its characteristics (temperature and electronic density, among
391 others). Using SEM analysis and laser pulse energy optimized for analyses of
392 waste PCBs, some parameters were obtained from the laser-waste PCB pellet
393 interaction.

394 The crater formed by the laser pulse over the surface of the pelletized
395 waste PCB sample S2 (200 mg compressed using $10x10^4$ N for 2 min) is shown
396 in Figure 2. The estimated crater diameter was 470 µm. The figure shows the

heterogeneity of the morphology and composition of the sample since waste PCBs consist of several polymeric, ceramic and metallic components. The importance of a milling step to obtain a representative sample and thus enable a stoichiometric ablation is also evident, besides the need to obtain several spectra in different regions of the pelletized sample for precision in determination (low RSD values). The laser-sample interaction is complex and many phenomena occur as a result.

The irradiance (W cm^{-2}) and the laser pulse fluence (J cm^{-2}) were calculated from the diameter of the crater. Using a laser pulse of 42.5 mJ and a pulse duration of 7.7 ns, a power of 5.5 MW was generated. Even if low energies are used, it is common to obtain high power values because the pulse duration lasts for nanoseconds. The crater radius reached 235 μm, obtaining an irradiance of 3.2 GW cm^{-2} and a laser fluence of 24.5 J cm^{-2}. These parameters were calculated for the optimized instrumental conditions used to obtain all the LIBS spectra for the waste PBC samples.

3.3. Evaluation of calibration strategies for LIBS

The matrix effects are the main sources of the linearity deviations between concentration and emission intensity in the analysis of solids by LIBS aimed at elementary determination. Thus, five calibration strategies (i- MMC, ii- TP CT, iii- OP MLC, iv- SSC and v- CF) were evaluated to overcome or minimize matrix effects in the determination of Al and Pb in six waste PCBs by LIBS. The criterion for selecting the analytes emission lines (λ) used in each calibration strategy was made considering the accuracy of the determinations based on the recovery value. Recoveries values in the range of 80 to 120% were considered satisfactory for all the evaluated calibration strategies.

Using matrix-matching calibration for Al, a calibration curve (coefficient of determination: R^2= 0.8146) was obtained by monitoring the emission line Al I 396.15 nm in the following samples: S1, S2, S3 and S4. For the validation of the method, two samples with intermediate concentrations to the calibration standards (S5 and S6) were analyzed. Recoveries values of 99% and 116%, and relative standard deviation (RSD) values ≦4% were obtained, demonstrating the satisfactory accuracy of MMC for Al determinations (see Table 1).

For Pb, the calibration curve obtained monitoring the emission line Pb I 405.78 nm at samples S2, S3, S4 and S5, showed a good coefficient of determination (R^2= 0.8426) using the MMC strategy. For samples S1 and S6 (used for validation), good recoveries values of 102% and 111% and RSD ≦ 8% were obtained for Pb determinations by LIBS (see Table 2).

For two-point calibration transfer strategy, the S4 (13.4 ± 0.7 g kg^{-1} Al) and S1 (7.6 ± 0.6 g kg^{-1}Pb) samples were used as calibration standards for Al and Pb, respectively. Since only two calibration points ("concentrations") are used, the linearity and significance of the model can be verified from the test F, and in this case the ratio $F_{experimental}/F_{tabulated}$ was calculated. This ratio ≥10 demonstrated that the variances are statistically different (the quadratic mean of the regression is statistically different when compared with the quadratic mean of the residues), thus the model can be considered linear and statistically significative, and the TP CT can be used (Pereira and Pereira-Filho 2018). The ratio found for all samples analyzed for Al ranged from 7 to 416 and for Pb ratios of 5 to 116 were obtained, indicating that the models are linear and that two-point calibration is feasible.

For Al, recovery values ranging from 84 to 112% were obtained using TP CT, except for S1 (683%), S2 (125%) and S3 (61%). For Pb, recovery values ranging from 89 to 104% were obtained, except for sample S4 (132%) (Tables 1 and 2). It was not possible to determine Pb in the S3 sample using LIBS and TP CT (or any other calibration strategy evaluated), since the concentration in this sample (0.72 ± 0.09 g kg^{-1}Pb) is lower than the standard error (SE) calculated for the LIBS method (Table 3). RSD values ≦17% and ≦22% were obtained in the determinations of Al and Pb, respectively, using TP CT.

For one-point and multi-line calibration, the samples of waste PCBs used as solid standards for Al and Pb were S5 (10.2 ± 1 g kg^{-1} Al) and S2 (11.6 ± 0.8 g kg^{-1} Pb), respectively. Good linear models were obtained, with excellent coefficients of determination for Al (R^2 ranging from 0.9790 to 0.9960) and Pb (R^2= 1), using four atomic emission lines for Al and two lines for Pb.

For Al, recoveries values ranging from 78 to 109% were obtained using OP MLC, except for S3 (57%). For Pb, excellent recoveries values ranging from 83 to 103% were obtained for all the samples analyzed (Tables 1 and 2). The values of the experimental slopes calculated for the linear models do not present significant differences from the theoretical slope (see Tables 1 and 2), providing good values of recoveries and demonstrating a satisfactory accuracy of the determinations. RSD values ≦9% and ≦25% were obtained in the determinations of Al and Pb, respectively.

Using the single-sample calibration for Al determination, the emission lines and concentrations of Al and Pb for all the samples and standard were used, except for samples S1 and S3. For these two samples, the intensity of the

emission lines of Al, Pb and Mg and the respective concentrations of these elements in the calibration standard were used. Recoveries values ranging from 82 to 116% were obtained using SSC, except for S1 (220%).

However, for Pb determination the emission intensity of the Pb, Al and Mg lines was used for all the waste PCB samples, together with the respective concentration values of these three elements in the calibration standard, except for sample S1. Only the Pb and Mg elements were monitored for this sample, together with their respective concentrations in the standard for correlation with the S1 sample. Recoveries values ranging from 81 to 116% were obtained using SSC, except for S6 (71%) - see Table 2. Using the SSC as a calibration strategy, RSD values of ≦21% and ≦25% were obtained in the determinations of Al and Pb, respectively.

Calibration free was another strategy evaluated for the determination of the analytes in the complex and refractory waste PCB samples. For CF it is necessary to obtain some physical parameters of the plasma, such as the temperature and electronic density, to verify the local thermodynamic equilibrium (LTE) (Ciucci et al. 1999, Tognoni et al. 2010).

For the calculation of the plasma temperature using the Saha-Boltzmann equation, the emission intensities of different lines in different ionization states (atomic and ionic) for Ba, Fe and Ti were used. The average plasma temperature was 8145 ± 227 K, considering the six waste PCB samples analyzed. The physical parameters of all the elements evaluated in the CF-LIBS are shown in Table S2, see supplementary material.

The electron density was calculated from the collision-induced enlargement of the Balmer H_α line to the hydrogen. The average plasma

497 electron density was 0.65 ± 0.29 10^{17} cm^{-3}, considering all the samples
498 analyzed.

499 From these values obtained for the temperature and electronic density
500 of the plasma (McWhirter criterion) (Tognoni et al. 2010) it is possible to assure
501 the existence of LTE in all the samples analyzed. Thus, also taking into account
502 stoichiometric ablation and using optically thin plasma, the concentration of Al
503 and Pb in the samples can be determined.

504 For Al, excellent recovery values ranging from 90 to 106% were
505 obtained using CF for all the samples analyzed. The recovery values for Pb
506 ranged from 78 to 121%, except for S6 (162%) - see Tables 2 and 3. RSD
507 values of ≦26% were obtained in Al and Pb determinations.

508 Some parameters related to the analytical performance and processing
509 of the data used for each of the evaluated calibration strategies are shown in
510 Table 3. It is interesting to observe how these parameters and the processing of
511 the spectra can change depending on the calibration strategy (SE and RMSEP,
512 for example). This is an indication of how matrix effects can be minimized by
513 using appropriate data processing and calibration strategies.

514 From the equations of the linear regression of the validation set (ICP
515 OES concentration reference *versus* LIBS predicted concentration plot), it is
516 possible to see that, in almost all cases the values, considering the confidence
517 interval, that the for the angular coefficient interval includes the number 1 and
518 the intercept includes the number 0, see Figures S1 and S2 in supplementary
519 material.

520 ### 3.4. What is the best calibration strategy for the determination of Al and
521 Pb in waste PCBs by LIBS?

In the plasma induced by LIBS, physicochemical phenomena and matrix effects occur during and due to laser-sample interaction, which in turn act on the atomic emission of the analytes, directly influencing the determination of Al and Pb in the samples of waste PCBs. However, with the data obtained from the evaluated calibration strategies, it can be seen that some of these strategies were very efficient, producing results with satisfactory accuracy. It can also be seen that the intrinsic properties of each analyte and of each calibration strategy directly influence the choice of the best calibration strategy.

The matrix-matching calibration gave excellent results for the determination of both analytes, with satisfactory recovery and RSD values. The MMC proved to be an efficient calibration strategy for the analysis of solids by LIBS, because since a set of waste PCB samples were used as calibration standards, the possible matrix effects are minimized when the physical properties of the calibration standards are close to those of the analyzed samples.

One limitation of the use of MMC in this study is that there is no set of certified reference materials (CRM) of waste PCBs, with reference values for Al and Pb, which could be used as solid standards when obtaining the calibration curve. Few initiatives are observed in the literature in order to produce a reference material for WEEE and a good example was published by Andrade et al. 2019a, 2019c. Thus, it was necessary to first obtain reference values of the analytes by analyzing a set of samples by a reference technique (in this study an ICP OES was used) for use as calibration standards for the LIBS method.

In some cases it is necessary to use vigorous conditions for the decomposition of the samples (high temperatures and high volume of

concentrated acid, as in this study). This represents a limitation in the use of MMC in the absence of adequate sample preparation instruments and reference values of the analytes required for later use of the samples as solid calibration standards for LIBS.

Two-point calibration transfer requires only one calibration standard (CRM or one reference value sample) and one sample with unknown concentration to determine the analyte concentration. In this calibration strategy, each set of spectra obtained in the LIBS analysis for standard and sample are divided into two sets and subsequently summed (the number of spectra composing set 2 must have approximately two-fold the number of spectra of set 1) (Castro et al. 2020).

If the standard and the sample have similar physical properties (for efficient matrix-matching), and the concentration of the standard is close to that of the sample, TP CT minimizes the matrix effects and enables a high degree of accuracy when determining the analyte concentration in the sample, using only one calibration standard and one linear model with two points. Tables 1 and 2 show that good recoveries values (ranging from 80 to 120%) were obtained for Al and Pb, when the concentration of the standard used was close to the concentration of these analytes in the sample. For samples with concentrations very different from those of the standards used, there was an under- or over-estimation of the analyte concentration.

The TP CT is an interesting simple calibration strategy for LIBS analysis when there is not a great variability of analyte concentration in the analyzed samples and when a standard with an appropriate concentration similar to that of the samples is used. This situation can be achieved in routine analysis.

572 Another strategy evaluated was one-point and multi-line calibration - OP
573 MLC. Excellent results were obtained for all the determinations of Al (except for
574 sample S3) and Pb in the waste PCB samples by LIBS. The OP MLC requires
575 only one calibration standard and several lines of analyte emission to obtain the
576 linear model, which facilitates the implementation of this calibration strategy
577 when few solid calibration standards are available in the laboratory routine.
578 Extra care has to be taken when using the OP MLC to remove lines with low
579 intensity that present spectral interferences, since they can harm the linear
580 models and consequently the measurement accuracy (Hao et al. 2018).
581 The determination of Al and Pb was also evaluated using the single-
582 sample calibration method - SSC, which is another recent calibration strategy
583 for LIBS that uses only one sample as standard (reference). In this strategy, a
584 simple correlation calculation is necessary to determine the analyte
585 concentration in the sample with unknown concentration (Yan et al. 2019).
586 Using SSC, good recoveries values were obtained for both Al (except sample
587 S1) and Pb (except sample S6).
588 For the use of SSC, the extent of the matrix effects between the sample
589 and the standard should be considered the same for all elements present in the
590 LIBS-induced plasma sample and the standard, since a direct correlation
591 between the emission intensity and concentration of these elements will be
592 used for the determination of the analyte. In addition, it should be considered
593 that none of the emission lines used in the SSC (analyte emission lines and
594 other elements used in the correlation) present spectral interferences, so that
595 results can be obtained with satisfactory precision and recovery (Yan et al.
596 2019).

Finally, using calibration free (CF) it was possible to obtain good results with excellent accuracy for Al and Pb determinations, except for Al determination in sample S6, using direct analysis of waste PCB samples by LIBS.

Not requiring a calibration standard is an advantage of CF, which makes it an excellent calibration strategy for use in elemental determination by LIBS in complex samples difficult to decompose. However, the quality of data acquisition and treatment in CF is a critical factor for obtaining satisfactory results. It is necessary to ensure that the emission measurements are obtained in LTE in the plasma, that the physical parameters used are correctly obtained and calculated with precision, and that only emission lines free of spectral interferences and self-absorption are employed in CF. Despite it is a laborious calculation procedure, CF allows the achievement of good results.

In this context, it is evident that it is difficult to choose the best calibration strategy for the direct determination of Al and Pb in waste PCBs by LIBS, since it depends on many variables. However, a knowledge of the advantages and limitations of each calibration strategy and a consideration of some intrinsic characteristics (physicochemical properties) of the sample and the analytes can help in selecting the best strategy that efficiently overcomes matrix effects and enables determination with satisfactory accuracy.

Table 4 shows some characteristics, advantages and limitations of the five calibration strategies evaluated in this study. This may help the reader to choose and evaluate the best calibration strategy for LIBS that could be used in different analytical contexts.

It is worth noting that there seems to be a tendency in recently reported new calibration strategies for LIBS to use no or few calibration standards (only 1 or 2) and to increasingly explore the physicochemical parameters and correlations of concentrations of the species present in the plasma induced by laser in each sample analyzed. Examples are TP CT, OP MLC, SSC evaluated in this study and other strategies recently reported in the scientific literature such as MEC (Babos et al. 2018) and OP GSA (Babos et al. 2019, Castro et al. 2020) calibration.

3.5 Evaluation of Al and Pb concentrations in waste PCBs: economic and environmental questions

As mentioned previously, waste PCBs can contain high concentrations of valuable and toxic metals. The recycling and appropriate disposal of this waste can both provide a source of income and contribute to environmental protection. In this context, LIBS is an excellent analytical tool for the monitoring of metals in the waste and for the development of methods for the analysis of solids and the direct determination of Al and Pb present in PCBs.

Were calculated estimations of the commercial value (in US$) per ton of each of the six samples of waste PCBs analyzed, considering only the measured concentrations of Al (ranging from 3.1 to 55 g kg^{-1} Al) and Pb (ranging from 0.72 to 11.6 g kg^{-1} Pb). Considered the prices of 1803 US$ / tonne Al and 1919 US$ / tonne Pb quoted on the London Metal Exchange, the second world center for industrial metals trading (LME, 2019).

The commercial value per tonne of the analyzed samples, considering only the Al and Pb contents, range from 20 to 121 US$ / tonne of waste PCB (prices for the S1 and S2 samples, respectively). These are good prices for

samples that are considered waste, particularly as they apply only to two metals present in the waste. Other valuable metals may also be present and thus the market price per ton of waste PCBs may be higher.

Concerning the environmental question, only one sample (S3 PCB, 0.072% Pb) complies with the maximum concentration value allowed (0.1% Pb) by weight in homogeneous materials for Pb in WEEE under Directive 2011/65/EU (RoHS, 2011). The Pb concentration in the other samples is between 5 and 12 times above the maximum allowed value according to the normative instruction. This is worrying, since if these samples are inappropriately disposed of they may be a source of contamination in the environment because of the Pb metal content.

Conclusion

The choice of the best calibration strategy for the direct analysis of waste PCBs for LIBS when aiming to determine Al and Pb depends on the intrinsic properties of these analytes and samples, as well as the ability of each of the calibration strategies to overcome the various matrix effects. Of the five calibration strategies evaluated, MMC and CF generally allowed accurate values to be obtained for both analytes in all the samples. The LIBS technique presented itself as an excellent analytical tool in the fast, simple and direct monitoring of recyclable metals such as Al and Pb and also of potential for environmental contamination such as Pb, originating from WEEE (waste PCB). The Pb concentrations determined are of concern as only one sample was in accordance with the Directive 2011/65/EU.

Credit author statement

Diego Victor Babos: Conceptualization; Data curation; Formal analysis; Validation; Visualization; Roles/Writing - original draft; Writing - review & editing.

Andrés Cruz-Conesa: Conceptualization; Data curation; Formal analysis; Validation; Visualization; Roles/Writing - original draft; Writing - review & editing.

Edenir Rodrigues Pereira-Filho: Conceptualization; Formal analysis; Resources; Supervision; Visualization; Writing - review & editing.

Jesús Manuel Anzano: Formal analysis; Funding acquisition; Project administration; Resources; Supervision; Visualization; Writing - review & editing.

Declaration of Competing Interest

The authors declare that they have no known competing financial interests or personal relationships that could have appeared to influence the work reported in this paper.

Acknowledgements

The authors are grateful to the Conselho Nacional de Desenvolvimento Científico e Tecnológico (CNPq – grants 141311/2017-7, 305637/2015-0) for fellowships and financial support. This study was financed in part by the Coordenação de Aperfeiçoamento de Pessoal de Nível Superior - Brasil (CAPES) - Finance Code 001, the Government of Aragon, the Servicio General de Apoyo a la Investigación-SAI, UNIZAR & the European Base Found, proposal E23_17D, and the Spanish Ministry of Science and Innovation, proposal #CTM2017-82929-R. The authors are also grateful to the São Paulo Research Foundation (FAPESP, grants 2016/01513-0). We would like to thank

MSc. Daniel F. Andrade and Dr. Raquel C. Machado for donating the electronic waste reference material.

References

Andrade, D.F., Machado, R.C., Pereira-Filho, E.R., 2019a. Proposition of electronic waste as a reference material – part 2: homogeneity, stability, characterization, and uncertainties J. Anal. At. Spectrom. 34, 2402-2410. https://doi.org/10.1039/C9JA00284G

Andrade, D.F., Fortunato, F.M., Pereira-Filho, E.R., 2019b. Calibration strategies for determination of the In content in discarded liquid crystal displays (LCD) from mobile phones using laser-induced breakdown spectroscopy (LIBS). Anal. Chim. Acta 1061, 42-49. https://doi.org/10.1016/j.aca.2019.02.038

Andrade, D.F., Machado, R.C., Bacchi, M., Pereira-Filho, E.R., 2019c. Proposition of electronic waste as a reference material – part 1: sample preparation, characterization and chemometric evaluation. J. Anal. At. Spectrom. 34, 2394-2401. https://doi.org/10.1039/C9JA00283A

Andrade, D.F., Romanelli J.P., Pereira-Filho, E.R., 2019d. Past and emerging topics related to electronic waste management: top countries, trends, and perspectives. Environ. Sci. Pollut. Res. 26, 17135-17151. https://doi.org/10.1007/s11356-019-05089-y

Andrade, D.F., Pereira-Filho, E.R., Amarasiriwardena, D., 2020. Current trends in laser-induced breakdown spectroscopy: a tutorial review. Appl. Spectrosc. Rev., https://doi.org/10.1080/05704928.2020.1739063

Aquino, F.W.B., Paranhos, C.M., Pereira-Filho, E.R., 2016. Method for the production of acrylonitrile–butadiene–styrene (ABS) and polycarbonate (PC)/ABS standards for direct Sb determination in plastics from e-waste using laser-induced breakdown spectroscopy. J. Anal. At. Spectrom. 31, 1228-1233. https://doi.org/10.1039/C6JA00038J

Arshadi, M., Yaghmaei, S., Mousavi, S.M., 2018. Recycling organics from non-metallic fraction of waste printed circuit boards by a novel conical surface triboelectric separator. Resour. Conserv. Recy. 139, 298-306. https://doi.org/10.1016/j.resconrec.2018.08.013

Augusto, A.S., Castro, J.P., Sperança, M.A., Pereira-Filho, E.R., 2019. Combination of Multi-Energy Calibration (MEC) and Laser-Induced Breakdown Spectroscopy (LIBS) for Dietary Supplements Analysis and Determination of Ca, Mg and K. J. Braz. Chem. Soc. 30, 804-812. https://doi.org/10.21577/0103-5053.20180211.

Babos, D.V., Barros, A.I., Nóbrega, J.A., Pereira-Filho, E.R., 2019. Calibration strategies to overcome matrix effects in laser-induced breakdown spectroscopy: Direct calcium and phosphorus determination in solid mineral supplements. Spectrochim. Acta B 155, 90-98. https://doi.org/10.1016/j.sab.2019.03.010

Babos, D.V., Virgilio, A., Costa, V.C., Donati, G.L., Pereira-Filho, E.R., 2018. Multi-energy calibration (MEC) applied to laser-induced breakdown spectroscopy (LIBS). J. Anal. At. Spectrom. 33, 1753-1762. https://doi.org/10.1039/C8JA00109J

Baldé, C., Forti, V., Gray, V., Kuehr, R., Stegmann, P., The Global E-waste Monitor 2017: Quantities, Flows, and Resources. 2017.

Carvalho, A.A.C., Cozer, L.A., Luz, M.S., Nunes, L.C., Rocha, F.R.P., Nomura, C.S., 2019. Multi-energy calibration and sample fusion as alternatives for quantitative analysis of high silicon content samples by laser-induced breakdown spectrometry. J. Anal. At. Spectrom. 34, 1701-1707. https://doi.org/10.1039/C9JA00149B

Carvalho, G.G.A., Guerra, M.B.B., Adame, A., Nomura, C.S., Oliveira, P.V., Carvalho, H.W.P., Santos Jr, D., Nunes L.C., Krug, F.J., 2018a. Recent advances in LIBS and XRF for the analysis of plants. J. Anal. At. Spectrom. 33, 919-944. https://doi.org/10.1039/C7JA00293A

Carvalho, A.A.C., Leme, F.O., Luz, M.S., Oliveira, P.V., Nomura, C.S., 2018b. Internal standard fused glass beads for high silicon content sample analysis by laser-induced breakdown spectrometry. J. Anal. At. Spectrom. 33, 1243-1250. https://doi.org/10.1039/C8JA00112J

Carvalho, R.R.V., Coelho, J.A.O., Santos, J.M., Aquino, F.W.B., Carneiro, R.L., Pereira-Filho, E.R., 2015. Laser-induced breakdown spectroscopy (LIBS) combined with hyperspectral imaging for the evaluation of printed circuit board composition. Talanta 134, 278-283. https://doi.org/10.1016/j.talanta.2014.11.019

Castro, J.P., Babos, D.V., Pereira-Filho, E.R., 2020. Calibration strategies for the direct determination of rare earth elements in hard disk magnets using laser-induced breakdown spectroscopy. Talanta 208, 120443. https://doi.org/10.1016/j.talanta.2019.120443

Castro, J.P., Pereira-Filho, E. R., 2016. Twelve different types of data normalization for the proposition of classification, univariate and multivariate regression models for the direct analyses of alloys by laser-induced breakdown spectroscopy (LIBS). J. Anal. At. Spectrom. 31, 2005-2014. https://doi.org/10.1039/C6JA00224B

771 Cavalcanti, G.H., Teixeira, D.V., Legnaioli, S., Lorenzetti, G., Pardini, L.,
772 Palleschi, V., 2013. One-point calibration for calibration-free laser-
773 induced breakdown spectroscopy quantitative analysis. Spectrochim.
774 Acta B 87, 51-56. http://dx.doi.org/10.1016/j.sab.2013.05.016
775 Ciucci, A., Corsi, M., Palleschi, V., Rastelli, S., Salvetti, A., Tognoni, E.,1999.
776 New Procedure for Quantitative Elemental Analysis by Laser-Induced
777 Plasma Spectroscopy. Appl. Spectrosc. 53, 960-964.
778 https://www.osapublishing.org/as/abstract.cfm?URI=as-53-8-960
779 Costa, V.C., Castro, J.P., Andrade, D.F., Babos, D.V., Garcia, J.A., Sperança,
780 M.A., Catelani, T.A., Pereira-Filho, E.R., 2018a. Laser-induced
781 breakdown spectroscopy (LIBS) applications in the chemical analysis
782 of waste electrical and electronic equipment (WEEE). Trends Anal.
783 Chem.108, 65-73. https://doi.org/10.1016/j.trac.2018.08.003
784 Costa, V.C., Augusto, A.S., Castro, J.P., Machado, R.C., Andrade, D.F., Babos,
785 D.V., Sperança, M.A., Gamela, R.R., Pereira-Filho, E.R., 2019. laser
786 induced-breakdown spectroscopy (LIBS): history, fundamentals,
787 applications and potentialities. Quim. Nova 42, 527-545.
788 http://dx.doi.org/10.21577/0100-4042.20170325
789 Costa, V.C., Babos, D.V., Aquino, F.W.B., Virgilio, A., Amorim, F.A.C., Pereira-
790 Filho, E.R., 2018b. Direct Determination of Ca, K and Mg in Cassava
791 Flour Samples by Laser-Induced Breakdown Spectroscopy (LIBS).
792 Food Anal. Methods 11, 1886-1896. https://doi.org/10.1007/s12161-
793 017-1086-9
794 Cremers, D.A., Radziemski, L.J., Handbook of laser-induced breakdown
795 spectroscopy, Wiley, London, 2006a.
796 Cremers D. A., Radziemski, L. J., History and fundamentals of LIBS, in:
797 Miziolek, A.W., Palleschi, V., Schechter, I., (Eds.), Laser-Induced
798 Breakdown Spectroscopy, Cambridge University Press, New York,
799 2006b
800 Derringer, G., Suich, R., 1980. Simultaneous Optimization of Several Response
801 Variables. J. Qual. Technol.12, 214-219.
802 https://doi.org/10.1080/00224065.1980.11980968
803 Eppler, A.S., Cremers, D.A., Hickmott, D.D., Ferris, M.J., Koskelo, A.C., 1996.
804 Matrix Effects in the Detection of Pb and Ba in Soils Using Laser-
805 Induced Breakdown Spectroscopy. Appl. Spectrosc. 50, 1175-1181.
806 https://doi.org/10.1366/0003702963905123
807 Fortunato, F.M., Catelani, T.A., Pomares-Alfonso, M.S., Pereira-Filho, E.R.,
808 2019. Application of Multi-energy Calibration for Determination of
809 Chromium and Nickel in Nickeliferous Ores by Laser-induced
810 Breakdown Spectroscopy. Anal. Sci. 35,165-168.
811 https://doi.org/10.2116/analsci.18P286

Gomes, M.S., de Carvalho, G.G.A., Junior, D.S., Krug, F.J., 2013. A novel strategy for preparing calibration standards for the analysis of plant materials by laser-induced breakdown spectroscopy: A case study with pellets of sugar cane leaves. Spectrochim. Acta B 86, 137-141. https://doi.org/10.1016/j.sab.2013.03.009

Gondal M.A., Seddigi, Z.S., Nasr, M.M., Gondal, B., 2010. Spectroscopy detection of health hazardous contaminants in lipstick using Laser induced breakdown spectroscopy, J. Hazard Mater. 175, 726-732. https://doi.org/10.1016/j.jhazmat.2009.10.069

Hahn, D.W., Omenetto, N., 2010. Laser-Induced Breakdown Spectroscopy (LIBS), Part I: Review of Basic Diagnostics and Plasma-Particle Interactions: Still-Challenging Issues within the Analytical Plasma Community. Appl. Spectrosc., 2010, 64, 335-366. https://doi.org/10.1366/000370210793561691

Hahn, D.W., Omenetto, N., 2012. Laser-Induced Breakdown Spectroscopy (LIBS), Part II: Review of Instrumental and Methodological Approaches to Material Analysis and Applications to Different Fields. Appl. Spectrosc. 66, 347-419. https://doi.org/10.1366/11-06574

Hao, Z.Q., Liu, L., Zhou, R., Ma, Y.W., Li, X.Y., Guo, L.B., Lu, Y.F., Zeng, X.Y., 2018. One-point and multi-line calibration method in laser-induced breakdown spectroscopy. Opt. Express 26, 22926-22933. https://doi.org/10.1364/OE.26.022926

Kim, G., Kwak, J., Kim, K.R., Lee, H., Kim, K.W., Yang, H., Park, K., 2013. Rapid detection of soils contaminated with heavy metals and oils bylaser induced breakdown spectroscopy (LIBS), J. Hazard Mater. 263, 754-760. http://dx.doi.org/10.1016/j.jhazmat.2013.10.041

Lasheras, R.J., Bello-Gálvez, C., Anzano, J. M., 2013. Quantitative analysis of oxide materials by laser-induced breakdown spectroscopy with argon as an internal standard. Spectrochim. Acta B 82, 65-70. https://doi.org/10.1016/j.sab.2013.01.005

Lasheras, R.J., Bello-Gálvez, C., Rodríguez-Celis, E.M., Anzano, J., 2011. Discrimination of organic solid materials by LIBS using methods of correlation and normalized coordinates, J. Hazard Mater. 192, 704-713. https://doi.org/10.1016/j.jhazmat.2011.05.074

Lednev, V. N., Grishin, M.Y., Sdvizhenskii, P.A., Asyutin, R.D., Tretyakov, R. S., Stavertiy, A.Ya., Pershin, S. M., 2019. Sample temperature effect on laser ablation and analytical capabilities of laser induced breakdown spectroscopy. J. Anal. At. Spectrom. 34, 607-615. https://doi.org/10.1039/C8JA00348C

Li, T., Hou, Z., Fu, Y., Yu, J., Gu, W., Wang, Z., 2019. Correction of self-absorption effect in calibration-free laser-induced breakdown spectroscopy (CF-LIBS) with blackbody radiation reference. Anal. Chim. Acta 1058, 39-47. https://doi.org/10.1016/j.aca.2019.01.016

London Metal Exchange - LME. https://www.lme.com/, 2019

Miziolek, W., Palleschi, V., Schechter, I., Laser induced breakdown spectroscopy. Cambridge University Press, Cambridge, 2006.

Morais, C.P., Barros, A.I., Bechlin, M.A., Silva, T.V., Santos Júnior, D., Senesi, G.S., Crespi, M.S., Ribeiro, C.A., Gomes Neto, J. A., Ferreira, E. C., 2018. Laser-induced breakdown spectroscopy determination of K in biochar-based fertilizers in the presence of easily ionizable element. Talanta, 188, 199-202. https://doi.org/10.1016/j.talanta.2018.05.089

NIST electronic database, https://www.nist.gov/pml/atomic-spectra-database

Pereira, F.M.V., Pereira-Filho., E.R., 2018. Application of free computational program in experimental design: a tutorial. Quim. Nova 41, 1061-1071. http://dx.doi.org/10.21577/0100-4042.20170254

Perkins, D.N., Drisse, M.-N.B., Nxele, T., Sly, P.D., 2014. E-Waste: A Global Hazard. Ann. Glob. Health 80, 286-295. http://doi.org/10.1016/j.aogh.2014.10.001

Popov, A.M., Zaytsev, S.M., Seliverstova, I.V., Zakuskin, A.S., Labutin, T.A., 2018. Matrix effects on laser-induced plasma parameters for soils and ores. Spectrochim. Acta B 148, 205-210. https://doi.org/10.1016/j.sab.2018.07.005

Restriction of Hazardous Substances Directive (RoHS) Directive 2011/65/EU Restriction of the Use of Certain Hazardous Substances in Electrical and Electronic Equipment, The European Parliament and the Council of the E. Union, 2011. http://data.europa.eu/eli/dir/2011/65/oj

Rezaei, A.H., Keshavarz, M.H., Tehrani, M.K., Darbani, S.M.R., 2018. Quantitative analysis for the determination of aluminum percentage and detonation performance of aluminized plastic bonded explosives by laser-induced breakdown spectroscopy. Laser Phys. 28, 065605. https://doi.org/10.1088/1555-6611/aab660

Sattar, H., Sun, L., Imran, M., Hai, R., Wu, D., Ding, H., 2019. Effect of parameter setting and spectral normalization approach on study of matrix effect by laser induced breakdown spectroscopy of Ag–Zn binary composites. Plasma Sci. Technol. 21, 034019 https://doi.org/10.1088/2058-6272/aaf712

Sperança, M.A., Andrade, D.F., Castro, J. P., Pereira-Filho, E.R., 2019. Univariate and multivariate calibration strategies in combination with laser-induced breakdown spectroscopy (LIBS) to determine Ti on sunscreen: A different sample preparation procedure. Opt. Laser Technol. 109, 648-653. https://doi.org/10.1016/j.optlastec.2018.08.056

Sperança, M.A., Pomares-Afonso, M.S., Pereira-Filho, E.R., 2018. Analysis of Cuban nickeliferous minerals by laser-induced breakdown spectroscopy (LIBS): non-conventional sample preparation of powder samples. Anal. Methods.10, 533-540. https://doi.org/10.1039/C7AY02521A

Takahashi, T., Thornton, B., 2017. Quantitative methods for compensation of matrix effects and self-absorption in Laser Induced Breakdown Spectroscopy signals of solids. Spectrochim. Acta B 138, 31-42. https://doi.org/10.1016/j.sab.2017.09.010

Tansel, B., 2017. From electronic consumer products to e-wastes: Global outlook, waste quantities, recycling challenges. Environ. Int. 98, 35-45. https://doi.org/10.1016/j.envint.2016.10.002

Tognoni, E., Cristoforetti, G., Legnaioli, S., Palleschi, V., 2010. Calibration-Free Laser-Induced Breakdown Spectroscopy: State of the art. Spectrochim. Acta B 65, 1-14. doi:10.1016/j.sab.2009.11.006

Vieira, A.L., Silva, T.V., de Sousa, F.S.I., Senesi, G.S., Santos Júnior, D., Ferreira, E. C., Gomes Neto, J. A., 2018. Determinations of phosphorus in fertilizers by spark discharge-assisted laser-induced breakdown spectroscopy. Microchem. J. 139, 322-326. https://doi.org/10.1016/j.microc.2018.03.011

Wu, C., Sun, D.X., Su, M.G., Yin, Y.P., Han, W.W., Lu, Q.F., Dong, C.Z., 2019. Quantitative analysis of Pb in soil samples by laser-induced breakdown spectroscopy with a simplified standard addition method. J. Anal. At. Spectrom. 34, 1478-1484. DOI: 10.1039/c9ja00059c

Yamane, L.H., de Moraes, V.T., Espinosa, D.C.R., Tenório, J.A.S., 2011. Recycling of WEEE: Characterization of spent printed circuit boards from mobile phones and computers. Waste Manage. 31, 2553-2558. https://doi.org/10.1016/j.wasman.2011.07.006

Yan, R., Tang, Y., Zhu, Z., Hao, Z., Li, J., Yu, H., Yu, Y., Guo, L., Zeng, X., Lu, Y., 2019. Accuracy improvement of quantitative analysis for major elements in laser-induced breakdown spectroscopy using single-sample calibration. Anal. Chim. Acta 1064, 11-16. https://doi.org/10.1016/j.aca.2019.02.056

Yang, J., Wang, H., Zhang, G., Bai, X., Zhao, X., He, Y., 2019. Recycling organics from non-metallic fraction of waste printed circuit boards by a novel conical surface triboelectric separator. Resour. Conserv. Recy. 146, 264-269. https://doi.org/10.1016/j.resconrec.2019.03.008

Yi, R.X., Guo, L.B., Zou, X.H., Li, J.M., Hao, Z.Q., Yang, X. Y., Li, X.Y., Zeng, X.Y., Lu, Y.F., 2016. Background removal in soil analysis using laser-induced breakdown spectroscopy combined with standard addition method. Opt. Express 24, 2607-2618. https://doi.org/10.1364/OE.24.002607

Table captions

Table 1. Concentrations (mean ± standard deviation, g kg^{-1} Al, n=3) and recovery (%) for Al in PCB samples determined by LIBS using matrix-matching calibration (MMC), two-point calibration transfer (TP CT), one-point and multi-line calibration (OP MLC), single-sample calibration (SSC) and calibration free (CF).

Sample	ICP OES	MMC	TP CT	OP MLC		SSC		CF
	g kg^{-1}			Theoretical slope*	Experimental Slope	g kg^{-1}		
S1	3.1 ± 0.4	-	21.2 ± 3.6 (683)	0.30	0.28 ± 0.03	2.9 ± 0.3 (93)	6.8 ± 1.1 (220)	3.3 ± 0.1 (106)
S2	55 ± 3	-	68.9 ± 8.4 (125)	5.39	5.87 ± 0.11	59.8 ± 1 (109)	-	49.8 ± 9.2 (91)
S3	21.4 ± 0.6	-	13.0 ± 1.4 (61)	2.09	1.19 ± 0.07	12.1 ± 0.6 (57)	24.8 ± 5.1 (116)	21.4 ± 3.1 (100)
S4	13.4 ± 0.7	-	-	1.32	1.02 ± 0.08	10.4 ± 0.8 (78)	13.5 ± 1.4 (101)	13.1± 3.4 (98)
S5	10.2 ± 1	11.8 ± 0.1 (116)	11.4 ± 0.9 (112)	-	-	-	10.4 ± 2.1 (102)	10.0 ± 2 (98)
S6	15.2 ± 0.9	15.0 ± 0.5 (99)	12.7 ± 1.4 (84)	1.49	1.23 ± 0.05	12.6 ± 0.5 (83)	12.4 ± 0.6 (82)	13.6 ± 1.2 (90)

- : Samples used for calibration

*Theoretical slope: $slope = \frac{C_{analyte}}{C_{standard}}$

Table 2. Concentrations (mean ± standard deviation, g kg^{-1} Pb, n=3) and recovery (%) for Pb in PCB samples determined by LIBS using matrix-matching calibration (MMC), two-point calibration transfer (TP CT), one-point and multi-line calibration (OP MLC), single-sample calibration (SSC) and calibration free (CF).

Sample	ICP OES	MMC	TP CT	OP MLC		SSC	CF
	g kg^{-1}			Theoretical slope*	Experimental Slope	g kg^{-1}	
S1	7.6 ± 0.6	7.8 ± 0.5 (102)	-	0.655	0.574 ± 0.089	6.7 ± 1 (88)	7.3 ± 0.6 (96)	5.9 ± 0.6 (78)
S2	11.6 ± 0.8	-	11.6 ± 0.8 (100)	-	-	-	-	14.1 ± 3.6 (121)
S3	0.72 ± 0.09	-	<1.1	0.062	0.008 ± 0.002	<1.2	<1.7	<2.7
S4	4.7 ± 0.9	-	6.2 ± 0.1 (132)	0.405	0.413 ± 0.029	4.8 ± 0.3 (103)	5.4 ± 0.3 (116)	5.5 ± 0.8 (116)
S5	10.7 ± 0.6	-	9.5 ± 2.1 (89)	0.922	0.766 ± 0.059	8.9 ± 0.7 (83)	8.6 ± 2.1 (81)	10.3 ± 2.2 (97)
S6	6.9 ± 1.6	7.6 ± 0.6 (111)	7.2 ± 0.9 (104)	0.595	0.611 ± 0.160	7.1 ± 1.8 (103)	4.9 ± 0.8 (71)	11.2 ± 2.2 (162)

- : Samples used for calibration

*Theoretical slope: $slope = \frac{C_{analyte}}{C_{standard}}$

Table 3. Analytical performance parameters

Parameter	Matrix-matching calibration	Two-point calibration transfer	Calibration free	One point and multi-line calibration		Single-sample calibration
Emission line (nm)	Al I 396.15 Pb I 405.78	Al I 396.15 Pb I 405.78	Several lines*	Al I 308.21 Al I 309.27 Al I 394.40 Al I 396.15	Pb I 363.95 Pb I 405.78	Al I 396.15 Pb I 405.78 Mg II 279.55
Normalization selected						
Al	Each individual spectrum is divided by its Euclidean norm and the average is calculated	Sum	Average of the spectra	Each individual spectrum is divided by its Euclidean norm, and the average is calculated		Each individual spectrum is divided by its Euclidean norm and the average is calculated
Pb	Average of the spectra	Sum	Average of the spectra	Average of the spectra		Average of the spectra
Signal type						
Al	Height	Height	Area	Height		Area
Pb	Height	Height	Area	Area		Height
SE (g kg^{-1})						
Al	1.6	12.2	2.4	5.6		2.9
Pb	0.76	1.1	2.7	1.2		1.7
RMSEP (g kg^{-1})						
Al	1.1	10.9	2.2	5.0		2.6
Pb	0.49	0.87	2.4	0.91		1.3
RSD range (%)						
Al	1 - 4	8 - 17	3 - 26	2 - 9		5 - 21
Pb	6 - 8	2 - 22	10 - 26	6 - 25		6 - 25

* see Table S2 in Electronic Supplementary Information (ESI).

Table 4. Advantages and limitations of the calibration strategies evaluated in this study for the determination of Al and Pb in waste PCBs by LIBS.

Calibration Method	Number of emission lines	Number of reference standard	Advantages	Limitations	Reference
Matrix-matching calibration	One	Between four and five	Efficient matching of the physical properties of the calibration standards with the samples	Difficulty in obtaining a set of commercial CRM or samples with reference values	Vieira et al. 2018, this study
Calibration free	Several	Not necessary	Does not require the use of calibration curves or matrix-matched standards	Occurrences of lines with self-absorption and spectral interferences, which compromise the determinations, laborious calculations	Tognoni et al. 2010, this study
One point and multi-line calibration	Several	One	Requires only one calibration standard	The choice of the standard with appropriate concentration, and the use of emission lines with low sensitivities	Hao et al. 2018, this study
Two-point calibration transfer	One	One	Simplicity in data processing and measurement accuracy	The choice of the standard with appropriate concentration as samples, and standards should show little variability between analyte concentrations	Castro et al. 2020, this study
Single-sample calibration	The number of lines of analytes present in the sample shall be ≤ to the number of lines used of the elements in the standard	One	No calibration curve or linear calibration model required	Samples and standards with significant variability of physico-chemical properties and analyte emission lines and reference elements with spectral interferences	Yan et al. 2019, this study

Figure captions

Figure 1. Scheme representation of the calibration strategies evaluated for direct determination of Al in waste PCBs by LIBS.

Figure 2. Crater and superficial morphology of waste PCB sample (S2) obtained by scanning electron microscopy (SEM).

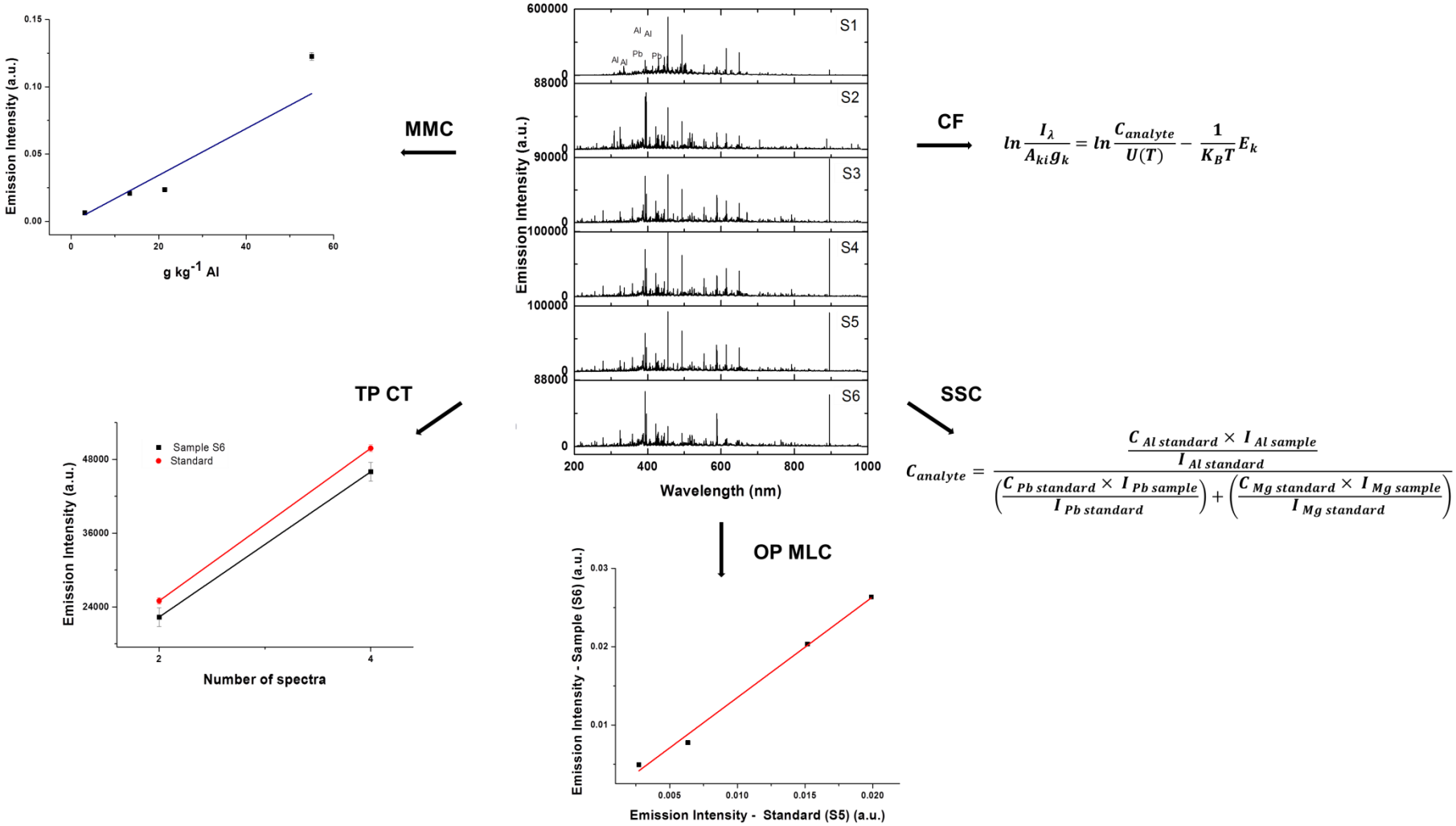

$$ln\frac{I_\lambda}{A_{ki}g_k} = ln\frac{C_{analyte}}{U(T)} - \frac{1}{K_B T}E_k$$

$$C_{analyte} = \frac{\frac{C_{Al\ standard} \times I_{Al\ sample}}{I_{Al\ standard}}}{\left(\frac{C_{Pb\ standard} \times I_{Pb\ sample}}{I_{Pb\ standard}}\right) + \left(\frac{C_{Mg\ standard} \times I_{Mg\ sample}}{I_{Mg\ standard}}\right)}$$

Figure 1

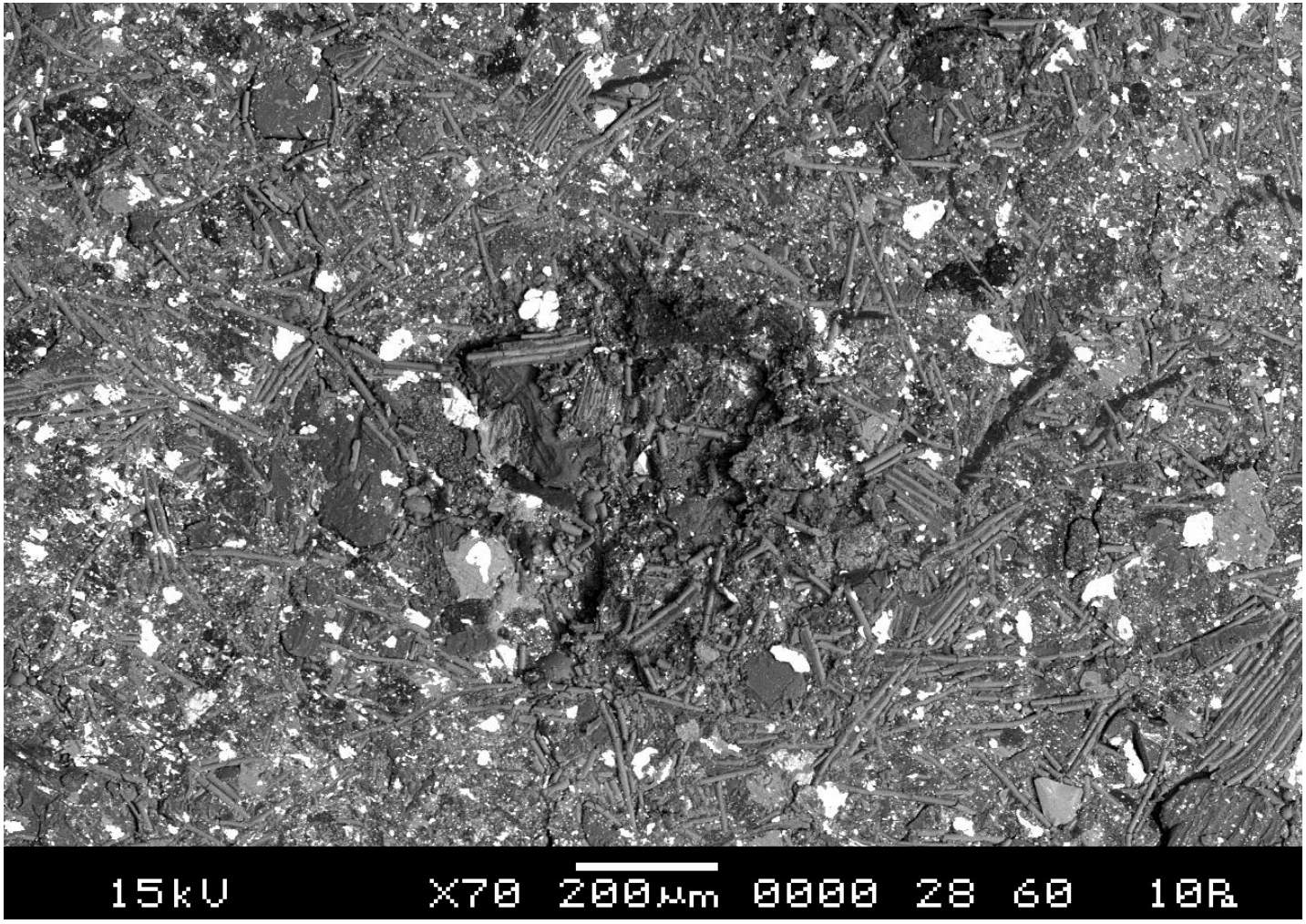

Figure 2

Electronic Supplementary Information (ESI):

Direct determination of Al and Pb in waste printed circuit boards (PCB) by Laser-induced breakdown spectroscopy (LIBS): evaluation of calibration strategies and economic - environmental questions

Diego Victor Babos,[1,2] Andrés Cruz-Conesa,[1] Edenir Rodrigues Pereira-Filho[2] and Jesús Manuel Anzano[1*]

[1]Laser Laboratory, Chemistry & Environment Group, Department of Analytical Chemistry, Faculty of Sciences, University of Zaragoza, Pedro Cerbuna 12, 50009 Zaragoza, Spain

[2]Group of Applied Instrumental Analysis, Department of Chemistry, Federal University of São Carlos, São Carlos, São Paulo State, 13565-905, Brazil

*Corresponding author:
Jesús Manuel Anzano
Laser Laboratory, Chemistry & Environment Group, Department of Analytical Chemistry, Faculty of Sciences, University of Zaragoza, Pedro Cerbuna 12, 50009 Zaragoza, Spain
Phone number: +34 9 7676 2684
E-mail: janzano@unizar.es (J. Anzano).

This ESI contains:

- 2 Tables
- 2 Figures

Table S1. Matrix of experiments showing the variables evaluated for optimizing delay time, gate width and laser pulse energy in LIBS determinations. The overall desirability (OD) was used as experimental response.

Experiment		Delay time (μs)		Gate width (μs)		Laser pulse energy (mJ)		OD
		Real	Coded	Real	Coded	Real	Coded	
Full factorial design 2^3	1	0.4	-1	1.0	-1	25	-1	0.49
	2	2.0	1	1.0	-1	25	-1	0.73
	3	0.4	-1	3.0	1	25	-1	0.67
	4	2.0	1	3.0	1	25	-1	0.55
	5	0.4	-1	1.0	-1	42.5	1	0.57
	6	2.0	1	1.0	-1	42.5	1	0.62
	7	0.4	-1	3.0	1	42.5	1	0.30
	8	2.0	1	3.0	1	42.5	1	0.89
Central point	9	1.2	0	2.0	0	35	0	0.44
	10	1.2	0	2.0	0	35	0	0.56
	11	1.2	0	2.0	0	35	0	0.77
	12	1.2	0	2.0	0	35	0	0.61
	13	1.2	0	2.0	0	35	0	0.62
Axial point	14	0.01	-1.49	2.0	0	35	0	0.41
	15	2.54	1.68	2.0	0	35	0	0.74
	16	1.2	0	0.32	-1.68	35	0	0.63
	17	1.2	0	3.68	1.68	35	0	0.64
	18	1.2	0	2.0	0	20	-1.68	0.69
	19	1.2	0	2.0	0	47.5	1.68	0.69

Table S2. Spectroscopic parameters λ (wavelength), E_i (energy of the lower level of transition), E_k (energy of the upper level of transition), A_{ki} (transition probability), and g_k (degeneracy factor of state k) of atomic (I) and ionic (II) lines used in the CF-LIBS calculation. Source: NIST DataBase.

Elements	**Line**	**λ (nm)**	**E_i (eV)**	**E_k (eV)**	**g_k**	**A_{ki} .10^8 (s^{-1})**
Al	I	309.271	0.01	4.02	6	0.730
Al	I	783.531	4.02	5.60	6	0.057
Al	I	783.613	4.02	5.60	6	0.004
Ba	II	614.172	0.70	2.72	4	0.412
Ba	II	649.690	0.60	2.51	2	0.130
Ba	I	705.994	1.19	2.95	9	0.500
C	I	247.856	2.68	7.68	3	0.180
Ca	II	317.933	3.03	7.05	6	3.600
Ca	I	558.876	40.05	43.51	7	0.409
Ca	I	612.222	1.89	3.91	3	0.287
Ca	I	616.217	1.90	3.91	3	0.477
Co	I	356.938	0.92	4.40	8	1.500
Cr	II	283.563	1.55	5.92	12	2.000
Cr	I	360.533	0.00	3.44	5	1.620
Cu	I	510.554	1.39	3.82	4	0.020
Cu	I	521.820	3.82	6.19	6	1.220
Cu	I	578.213	1.64	3.79	2	0.019
Fe	II	239.924	0.08	5.25	6	1.400
Fe	I	373.532	0.86	4.18	7	0.270
Fe	I	382.042	0.86	4.10	9	0.668
Fe	I	404.581	1.48	4.55	9	0.863
Fe	I	438.354	1.48	4.31	11	0.500
Mg	I	518.361	2.72	5.11	3	0.561
Mn	II	293.306	1.17	5.40	3	2.040
Ni	I	341.476	0.03	3.66	9	0.550
Ni	I	351.505	0.11	3.64	7	0.420
Ni	I	352.454	0.03	3.54	5	1.000
Pb	I	405.780	1.32	4.38	3	0.912
Sb	I	259.805	1.06	5.83	2	0.210
Si	I	288.158	0.78	5.08	3	1.890
Sn	I	317.050	0.42	4.33	3	0.838
Ti	II	334.941	0.05	3.75	12	1.680
Ti	I	498.173	0.85	3.34	13	0.660
Ti	I	499.107	0.84	3.34	11	0.584
Zn	I	481.053	4.08	6.65	3	0.700

Figure S1. Comparison of Al concentrations determined in waste PCBs samples by the proposed LIBS method using different calibration strategies (a- MMC, b- TP CT, c- OP MLC, d- SSC and e- CF) and the ICP OES reference method. The SE and RMSEP were added as lines parallel to the X-axis.

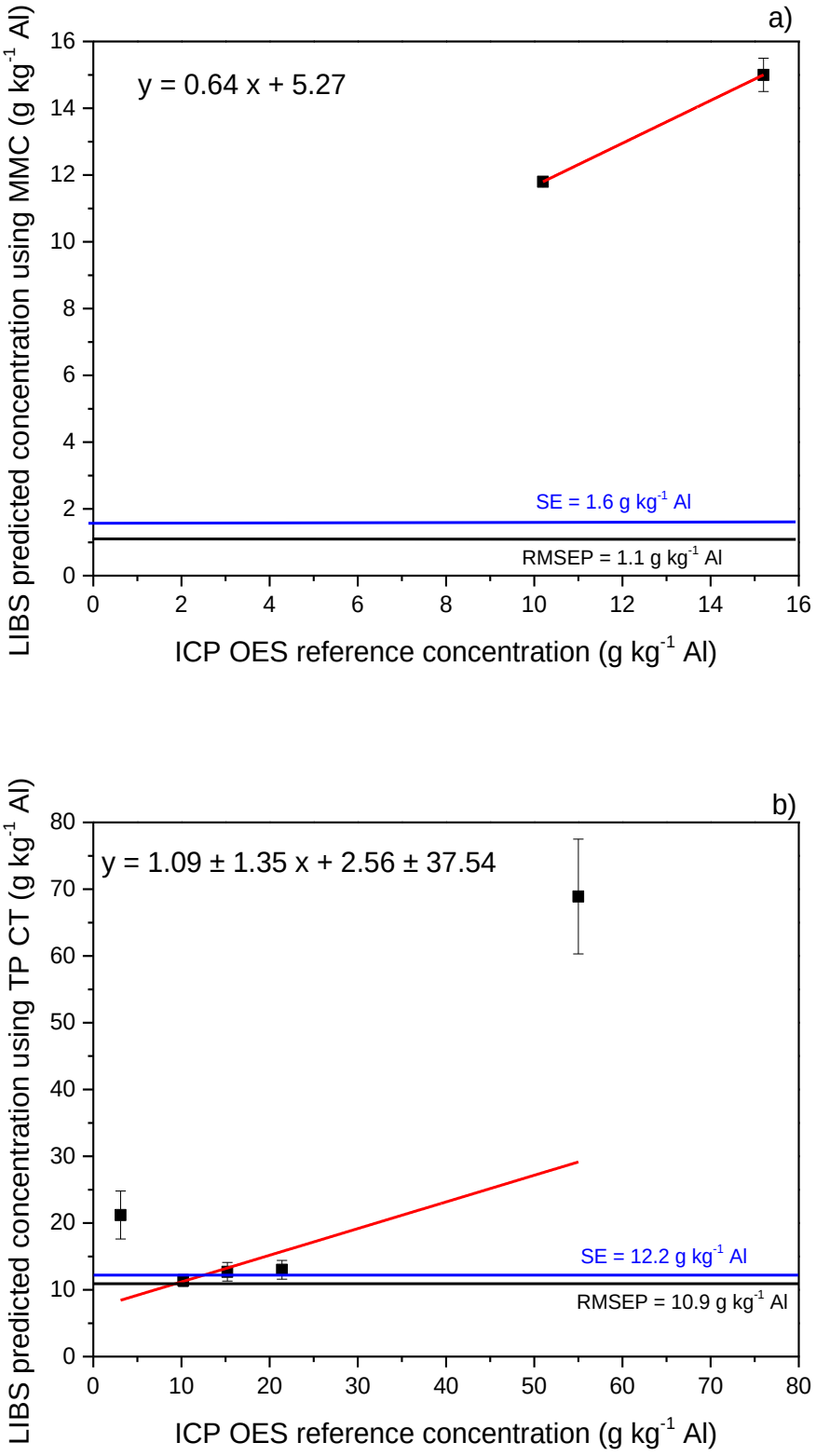

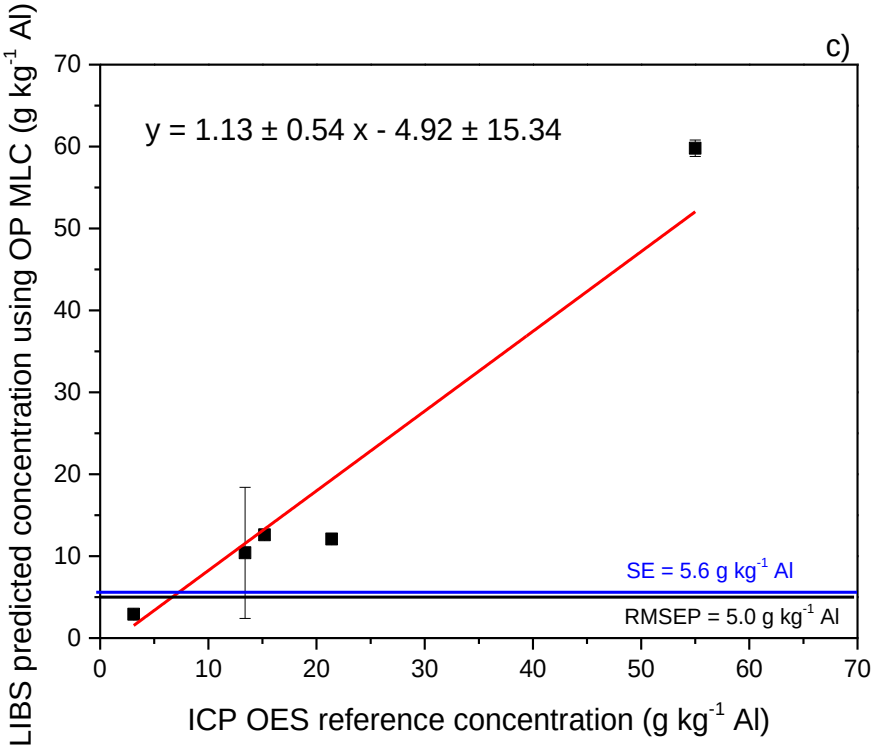
c)
y = 1.13 ± 0.54 x - 4.92 ± 15.34
SE = 5.6 g kg-1 Al
RMSEP = 5.0 g kg-1 Al
LIBS predicted concentration using OP MLC (g kg-1 Al)
ICP OES reference concentration (g kg-1 Al)
0
10
20
30
40
50
60
70

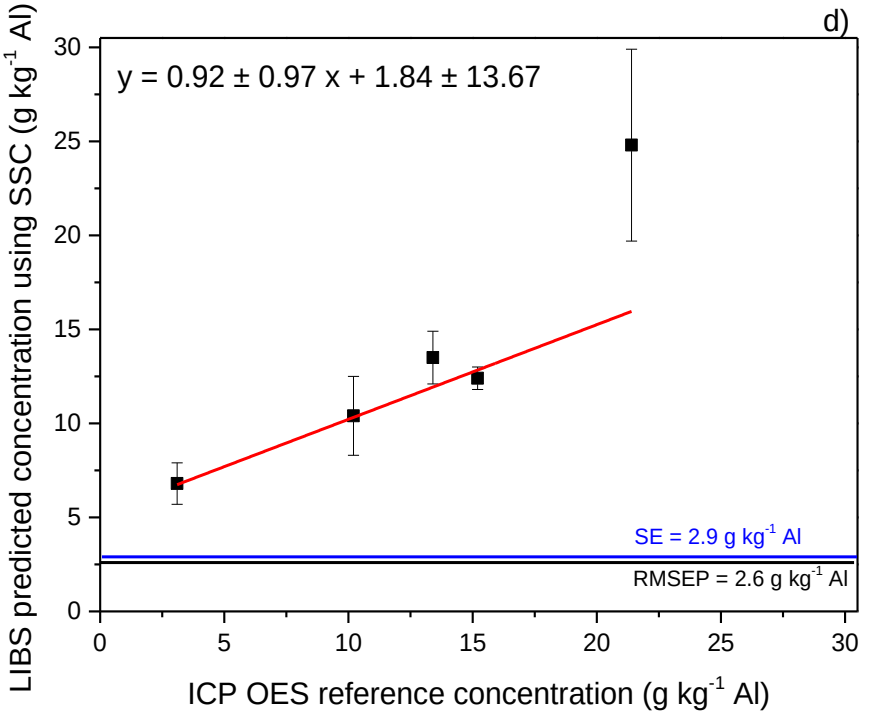
d)
y = 0.92 ± 0.97 x + 1.84 ± 13.67
SE = 2.9 g kg-1 Al
RMSEP = 2.6 g kg-1 Al
LIBS predicted concentration using SSC (g kg-1 Al)
ICP OES reference concentration (g kg-1 Al)
0
5
10
15
20
25
30

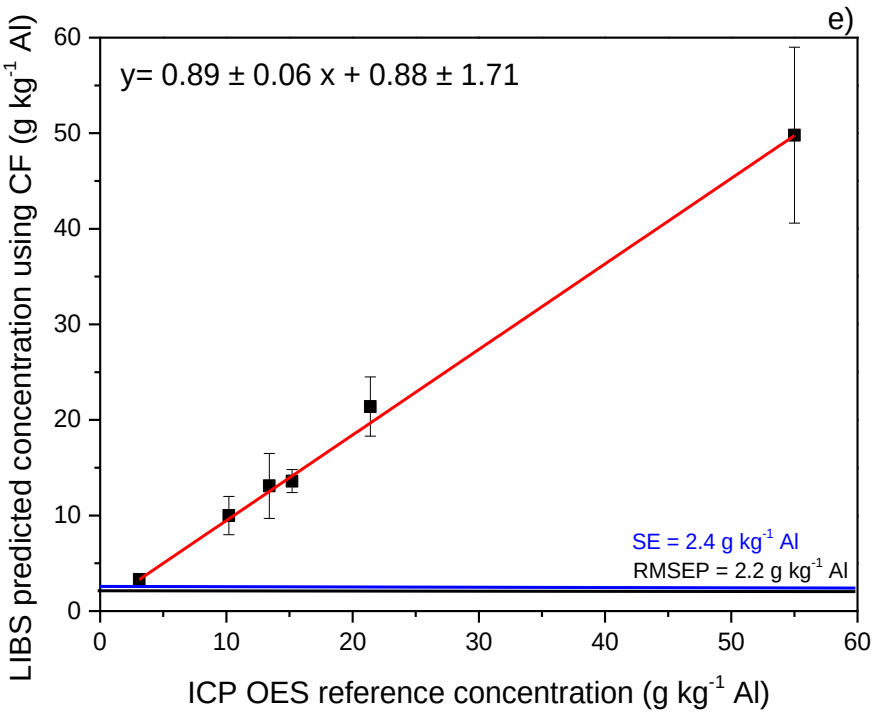
e)
y= 0.89 ± 0.06 x + 0.88 ± 1.71
SE = 2.4 g kg-1 Al
RMSEP = 2.2 g kg-1 Al
LIBS predicted concentration using CF (g kg-1 Al)
ICP OES reference concentration (g kg-1 Al)
0
10
20
30
40
50
60

Figure S2. Comparison of Pb concentrations determined in waste PCBs samples by the proposed LIBS method using different calibration strategies (a- MMC, b- TP CT, c- OP MLC, d- SSC and e- CF) and the ICP OES reference method. The SE and RMSEP were added as lines parallel to the X-axis.

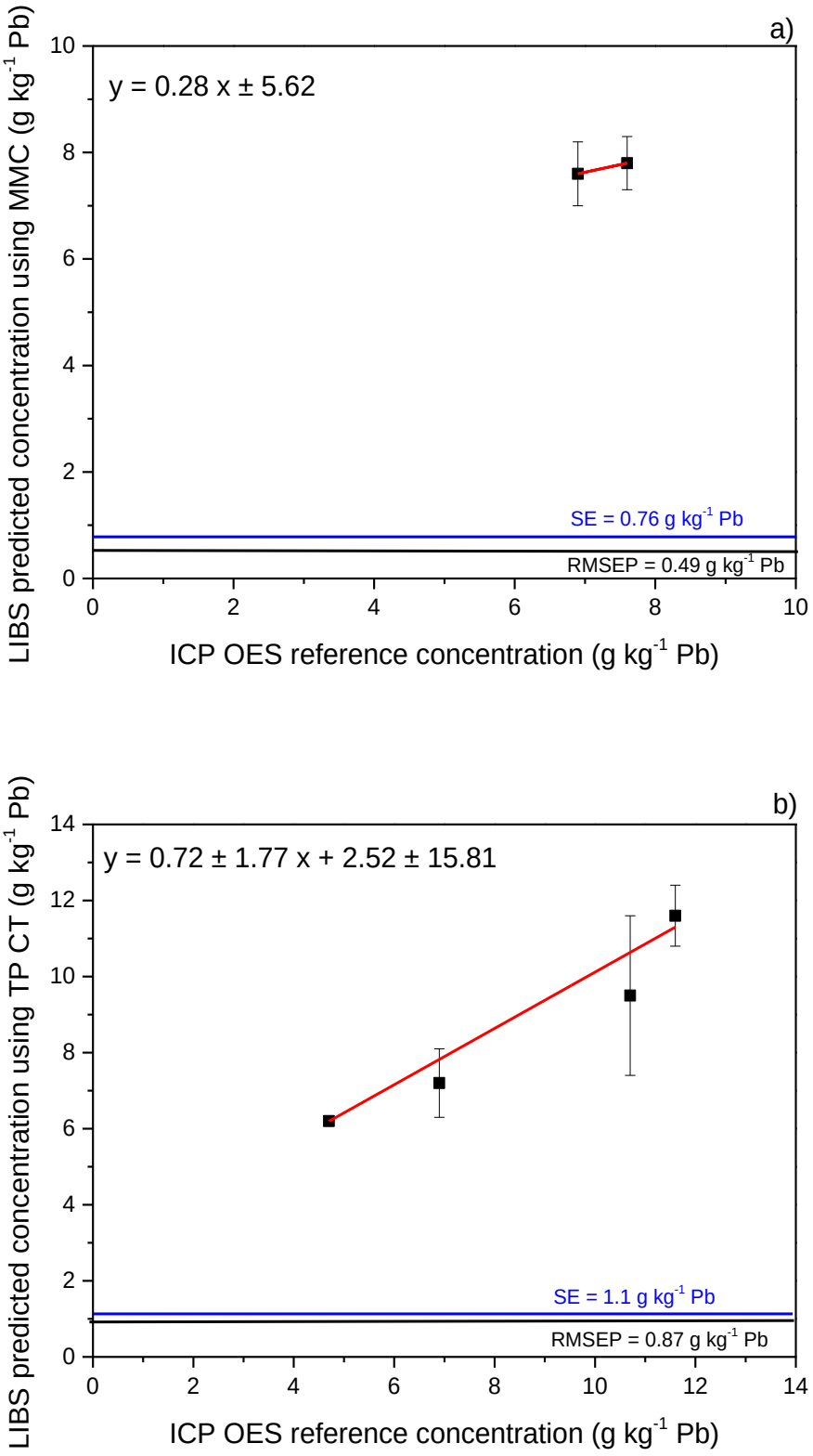

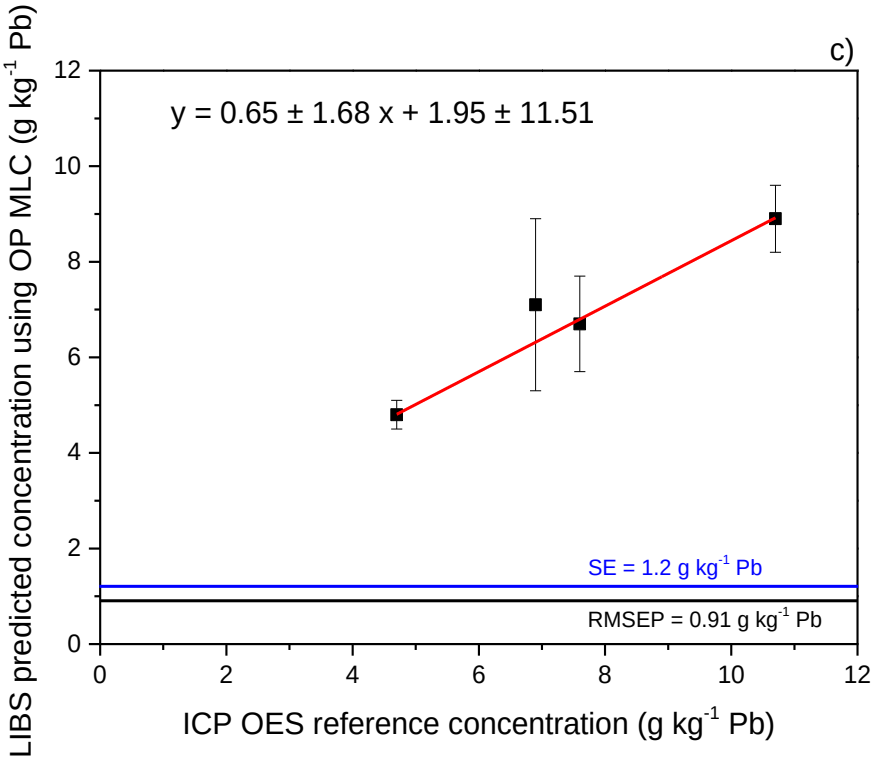
c)
y = 0.65 ± 1.68 x + 1.95 ± 11.51
SE = 1.2 g kg-1 Pb
RMSEP = 0.91 g kg-1 Pb
LIBS predicted concentration using OP MLC (g kg-1 Pb)
ICP OES reference concentration (g kg-1 Pb)
0
2
4
6
8
10
12

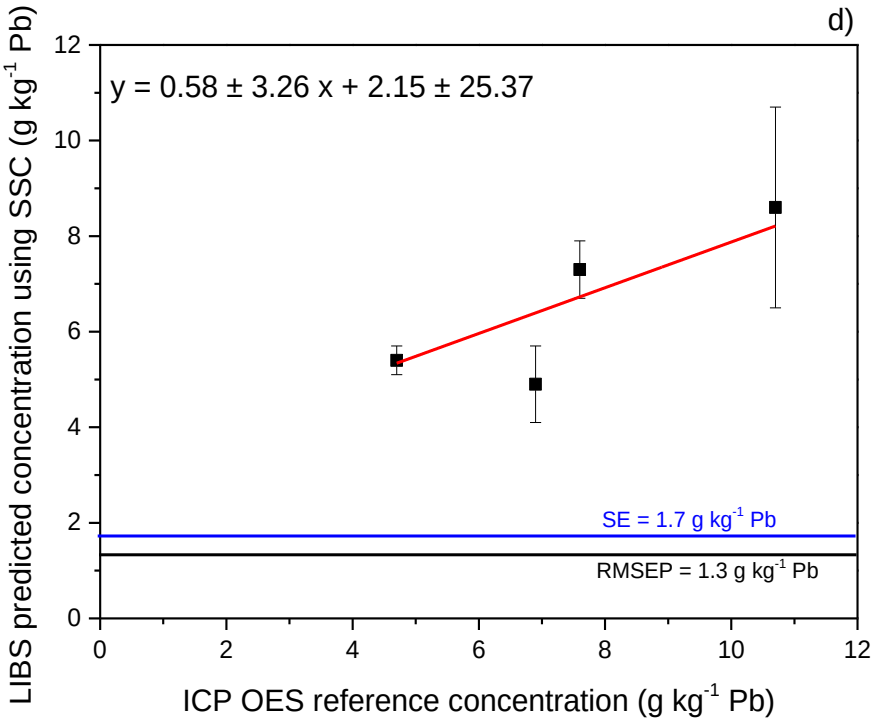
d)
y = 0.58 ± 3.26 x + 2.15 ± 25.37
SE = 1.7 g kg-1 Pb
RMSEP = 1.3 g kg-1 Pb
LIBS predicted concentration using SSC (g kg-1 Pb)
ICP OES reference concentration (g kg-1 Pb)
0
2
4
6
8
10
12

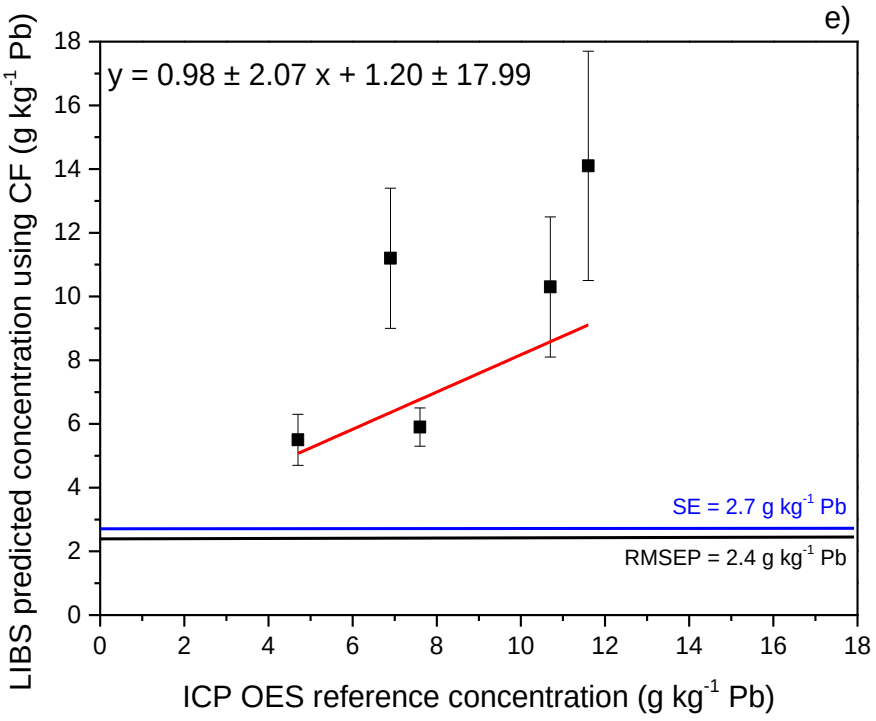
e)
y = 0.98 ± 2.07 x + 1.20 ± 17.99
SE = 2.7 g kg-1 Pb
RMSEP = 2.4 g kg-1 Pb
LIBS predicted concentration using CF (g kg-1 Pb)
ICP OES reference concentration (g kg-1 Pb)
0
2
4
6
8
10
12
14
16
18